

Chemical Recycling of Polyolefinic Waste to Light Olefins by Catalytic Pyrolysis

Niklas Netsch, Jonas Vogt, Frank Richter, Grazyna Straczewski, Gerd Mannebach, Volker Fraaije, Salar Tavakkol*, Shahram Mihan, and Dieter Stapf

DOI: 10.1002/cite.202300078

 This is an open access article under the terms of the Creative Commons Attribution-NonCommercial-NoDerivs License, which permits use and distribution in any medium, provided the original work is properly cited, the use is non-commercial and no modifications or adaptations are made.

Catalytic pyrolysis of post-industrial and post-consumer waste is studied in an auger-type reactor at pilot scale by applying two different zeolites and an amorphous silica-alumina catalyst in-situ at 400–550 °C. Contrary to thermal pyrolysis, of polyolefin-rich waste, high gaseous pyrolysis product yields of approx. 85 wt % are achieved with C₂–C₄ olefin contents of up to 67 wt %. After deactivation by coke deposition catalyst regeneration is proved feasible for maintaining the gaseous product yield and composition. Waste feedstocks with significant nitrogen and halogen heteroatom content are not suitable for in-situ catalytic pyrolysis.

Keywords: Chemical recycling, catalytic pyrolysis, mixed plastic waste, polyolefins-to-olefins, waste-to-chemicals

Received: April 27, 2023; *accepted:* June 15, 2023

1 Introduction

Resource scarcity and steadily increasing anthropogenic CO₂ emissions, as with the resulting consequences, such as political conflicts or global warming, are pushing for a rethink of the consumption of fossil resources [1,2]. Thus, the transformation from traditional linear value chains to a resource-efficient circular economy is considered an important upcoming challenge for industry and society [3–5]. In the chemical industry, renewable resources such as biomass [6] and the use of carbon dioxide as feedstock [7] are gaining momentum. Compared to these, the closed-loop approach to replace fossil feedstocks by increased plastic waste recycling is most promising in terms of energy demand [8], capital investment needs, and thus speed of implementation. However, in 2019 only 9 % of plastic waste was recycled worldwide, while a large share of the carbon bound in plastic waste was removed from a potential product cycle through landfilling and incineration [9]. Although the recycling quota within the European Union in 2018 is significantly higher than globally (33 %), there is still substantial potential for improvement, especially since recycling is almost exclusively accomplished by mechanical processing [10].

Due to the complex and heterogeneous composition of plastic waste along with its mechanical-thermal degradation during processing and use, many wastes are difficult to recycle into high-value products mechanically [11,12]. This issue can be addressed by applying chemical recycling complementary to mechanical recycling [13–15]. Hereof, thermal pyrolysis is a process with high feedstock flexibility capable of processing wastes with high content of hetero-

atoms such as nitrogen, sulfur, or chlorine. If the waste fraction consists mainly of polyolefins that represent most of the plastics products, catalyst-supported pyrolysis is an option to specifically enhance product yields and selectivities and thus enable even more efficient recycling [16,17].

Thermal pyrolysis of polyolefins is characterized by a radical chain scission mechanism leading to a broad distribution of hydrocarbons with a significant yield of waxy high boiling paraffins [18,19]. The elemental composition ensures the absence of heteroatom-containing hydrocarbons which is why the application of catalyst to the pyrolytic process is possible [20], even though an increased tendency to coke formation is reported especially in catalytic slow pyrolysis of polyolefinic waste in industrial-scale facilities [21]. In general, catalytic pyrolysis of polyethylene and polypropylene (PP) favors cracking, and thus, mostly light olefins and low-boiling paraffinic hydrocarbons are obtained. Both, yield and selectivity towards these valuable products can be controlled by the chemical and physical properties of the

¹Niklas Netsch  <https://orcid.org/0000-0002-2982-181X>,

¹Jonas Vogt, ¹Frank Richter, ¹Dr. Grazyna Straczewski

 <https://orcid.org/0000-0002-5172-7360>,

²Dr. Gerd Mannebach, ²Dr. Volker Fraaije, ¹Dr. Salar Tavakkol

 <https://orcid.org/0000-0001-5142-2439> (salar.tavakkol@kit.edu),

²Dr. Shahram Mihan, ¹Prof. Dr.-Ing. Dieter Stapf

 <https://orcid.org/0000-0001-6499-062X>

¹Karlsruhe Institute of Technology (KIT), Institute for Technical Chemistry (ITC), Hermann-von-Helmholtz-Platz 1, 76344 Eggenstein-Leopoldshafen, Germany.

²Basell Polyolefine GmbH, Industriepark Höchst, 65926 Frankfurt am Main, Germany.

catalyst, as well as by operating conditions. Furthermore, cracking catalysts, such as fluid catalytic cracking (FCC) catalysts, zeolites, and silica-alumina catalysts, accelerate endothermic cracking reactions by reducing the energy demand for chain scission of hydrocarbons depending on their characteristic properties [22].

For the pyrolysis of plastic waste, heterogeneous solid acid catalysts are considered because of their robustness, easy handling, and their reactivity [22–24]. FCC catalysts consist of zeolite crystals in a silica-alumina matrix whereas silica-alumina catalysts are characterized as amorphous solid acids [25]. By applying FCC catalysts in high-density polyethylene (HDPE) pyrolysis oil yields of up to 80 wt % can be achieved depending on the feedstock, the catalyst properties, and operating conditions [26]. In contrast, silica-alumina and zeolite catalysts increase the gas yields by up to 89 wt % and 94 wt % because of the enhanced selectivity to light hydrocarbon formation [18]. The selectivity can be adjusted by the pore structure, elemental catalyst composition, and the resulting acidity [27].

Zeolites are crystalline aluminosilicates, of which ZSM-5, zeolite Y, and zeolite beta are the most prominent examples. Their characteristic pore structure determines the access to reactive sites where cracking, or secondary reactions (e.g., oligomerization, cyclization, aromatization) occur [16, 28]. A molecular-sized pore structure, as present in medium pore ZSM-5 sterically hinders secondary bimolecular reactions to possible precursors of solid carbon components and provides high yields of light olefins and other primary products, compared to large pore zeolites, silica-alumina or FCC catalysts which show higher coke formation [29]. The reactive centers of the catalysts are acid sites, which can be modified by the $\text{SiO}_2/\text{Al}_2\text{O}_3$ ratio. A lower $\text{SiO}_2/\text{Al}_2\text{O}_3$ ratio results in a higher number of acid sites which shifts the product spectrum towards lighter hydrocarbons by end-chain scission of the long-chain hydrocarbons [30–32]. This correlation is reversed for amorphous silica-alumina as the acidity decreases with decreasing $\text{SiO}_2/\text{Al}_2\text{O}_3$ ratio [33]. Higher acidity enables the production of lighter hydrocarbons but also promotes coke formation leading to catalyst deactivation [34, 35].

The impact of the catalysts' properties has been investigated focusing on virgin plastics and polyolefinic waste fractions mainly in laboratory-scale studies [17–19, 22, 23, 26, 27, 29–31, 34, 36–40]. The catalyst application for pyrolysis of real waste plastics has been studied only to a limited extent on technical scale because of difficult process control due to feedstock heterogeneity, and the tendency of catalyst deactivation [24, 41, 42]. Therefore, the scope of this work is to investigate the catalytic pyrolysis of polyolefin-rich plastic wastes at a scalable reactor concept. Process engineering challenges, such as an appropriate catalyst and feedstock introduction, are studied.

2 Materials and Methods

2.1 Feedstock Description and Preparation

Focusing on polyolefins and polyolefin-rich waste various feedstocks are investigated in this study. These feedstocks can be distinguished among virgin plastics, post-industrial plastic waste (PIW), and post-consumer plastic waste (PCW). The virgin plastics low-density polyethylene (LDPE) and isotactic PP are additive-free primary granules with a cylindrical shape. Isotactic PP (Moplen HP522H) and low-density polyethylene (LDPE) (Lupolen 2420H) are supplied by Basell Polyolefine GmbH. PIW includes granules from used agricultural films (W1) and a waste fraction obtained from the production of multilayer packaging films (W2). W1 is primarily composed of LDPE, while W2 consists of polyethylene in combination with polyamide layers or layers of polyethylene terephthalate (PET) or ethylene vinyl alcohol (EVOH). Amounts of metallic or inorganic impurities are to be expected to a small extent. However, W2 contains significant quantities of organically bound nitrogen and oxygen due to film layers, while small residues of soil in the granules are conceivable for W1. As examples of PCW, two different mixed plastic waste fractions from state-of-the-art mechanical recycling facilities are investigated in this work. The first fraction represents a residue generated in a sensor-based mechanical sorting process (W3), while the other feedstock, as a light fraction of mechanical recycling, mainly includes two-dimensional packaging waste, such as films (W4). For W3 a high polyethylene, PP, polyamide, and PET content is expected. Particularly for W4, organic and inorganic impurities are to be expected.

Prior to pyrolysis of the feedstock, pretreatment is required depending on the type of material. While the PP, LDPE, and the PIW are delivered as homogeneous granules, the PCW must be homogenized and crushed to processable particle size. In the first step of the pretreatment procedure the PCW is shredded (Untha RS 30 and Retsch SM200) to a maximum diameter of 6 mm and then further homogenized by intensive manual mixing. Subsequently, the material is dried in an oven at 105 °C for 6 h. In order to increase the density and improve the transport behavior in the screw pyrolysis reactor, the shredded, homogenized, and dried waste is pelletized (Kahl Pelletpresse type 14-175). The feedstock material is characterized by an elemental analysis (DIN EN ISO 16948) after the required preconditioning steps. The moisture and ash content (DIN EN 14775) was determined beforehand. The results are listed in Tab. 1.

2.2 Catalysts

The catalysts used in the experiments are commercially available cracking catalysts provided as powder. Catalysts A and B belong to the catalyst group of microporous zeolites

Table 1. Moisture, ash content, and elemental composition of the feedstock after potential pretreatment.

	LDPE	PP	W1	W2	W3	W4
Particle shape	extrudate	extrudate	granule	extrudate	pellet	pellet
Diameter [mm]	5	5	5	7	7	7
Length [mm]	5	5	–	10	10	10
Moisture [wt.%] ^{a)}	0.0	0.0	0.0	0.7	0.0	0.4
Ash [wt.%] ^{b)}	< 0.1	< 0.1	2.4	< 0.6	2.1	9.6
<i>Elemental analysis</i>						
C [wt.%] ^{c)}	85.5	85.4	81.5	75.0	74.7	66.4
H [wt.%] ^{c)}	14.2	14.1	13.2	11.3	10.1	8.5
N [wt.%] ^{c)}	< 0.1	< 0.1	< 0.1	3.0	0.4	0.6
S [wt.%] ^{c)}	< 0.1	< 0.1	< 0.1	< 0.1	< 0.1	0.2
Cl [wt.%] ^{c)}	< 0.01	< 0.01	< 0.01	< 0.01	0.1	0.8
Br [wt.%] ^{c)}	< 0.01	< 0.01	< 0.01	< 0.01	< 0.01	< 0.01
O [wt.%] ^{c,d)}	0.3	0.5	2.9	10.7	12.6	13.5

a) Mass loss at 100 °C; b) residue of incineration at 550 °C; c) related to the dry feedstock; d) calculated as difference to 100 wt %.

but differ in terms of pore size and acidity, while catalyst C is classified as an amorphous silica-alumina hydrate. For proprietary reasons, the precise designation of the catalyst supplied and further information about their properties cannot be provided.

To ensure uniform catalyst dosing, the catalyst particles are applied homogeneously to the surface of quartz sand particles, which have a diameter of approx. 1 mm. The attachment of the catalyst layer to the sand surface is performed in two distinct methods. The simpler variant is the fixation by adhesion forces with the supplementary addition of paraffin oil. Therefore, quartz sand is mixed with paraffin oil and catalyst powder. Concerning the sand mass, 2 wt % of catalysts and 1 wt % of paraffin oil are applied. The more elaborate method is the permanent fixation of the catalyst particles on the surface of the quartz sand based on a silica binder. Therefore, sand, catalyst, and the precursor of the binder are homogeneously mixed and then calcined. Again, 2 wt % of catalyst is added to ensure comparability of the experiments. The resulting binder is inert and does not evaporate at room temperature, which enables temperature-stable fixation. Catalyst prepared according to the method of permanent fixation is marked with an apostrophe (e.g., B'). The fixation method by paraffin oil represents a scalable and more cost-effective solution for large-scale applications. In contrast to the fixation using silica binder, the paraffin oil evaporates in the reactor. Therefore, the sand-catalyst blend with silica binder offers a significant advantage for large-scale applications since it can be recycled multiply assuming that mechanical stress during conveyance through the reactor only slightly impairs the bond between the catalyst particles and the sand surface.

2.3 Reactor Setup and Experimental Procedure

The experiments are carried out using a pilot-scale auger-type reactor with integrated hot gas filtration. The reactor and the periphery are already described in detail by Zeller et al., Netsch et al. and Tomasi-Morgano et al. for thermal experiments with various waste materials [43–45]. In this work, the sand is replaced by the previously described sand-catalyst mixture. In addition to its function as a catalyst carrier material, the sand enhances the transport behavior and heat transfer within the reactor. The sand-catalyst mixture and the feedstock are dosed via separate hoppers and dosing systems. The isothermal reactor fluctuates in temperature by a maximum of 10 °C around the set point. Non-volatile components of the feedstock and pyrolysis char in combination with sand and catalyst are collected at the outlet of the reactor. Volatile products pass the ceramic hot gas filters located along the reactor's freeboard and are directly transferred to a condensation unit. Organic products condense in three stages (60 °C, 60 °C and –5 °C). Non-condensable gaseous products referred to as permanent gases are subsequently analyzed and discharged to a flare.

In the study, the feedstock is dosed in a mass ratio of 1:4 relative to the sand-catalyst mixture. Hence, the catalyst/feedstock ratio is 0.08 kg kg⁻¹. If not indicated otherwise, experiments are conducted under reference conditions, which implies a reactor temperature of 450 °C, a solids residence time in the reactor of 30 min, a feedstock flow rate of 1 kg h⁻¹, and a pressure of about 1 bar. The reactor is purged with about 19 L min⁻¹ of nitrogen. The minimal experimental duration of 5 h ensures steady-state operation of over 4 h. The suspended solids as well as the amount of feedstock

and sand-catalyst mixture introduced are weighed. Experiments with feedstocks containing significant oxygen result in formation of an aqueous pyrolysis product phase. This phase is separated from the organic phase and both condensate phases are weighed separately. With the continuous mass determination of the permanent gases the mass balance is derived.

2.4 Analytical Methods

The reactor temperature and pressure are continuously measured at various positions of the reactor system. In addition to the precise determination of the supplied nitrogen with mass flow controllers (Bronckhorst EL-FLOW Select), characteristic gas species such as CO, CO₂, CH₄, and O₂ (Siemens OXYMAT 6, Emerson X-Stream) are monitored for process control. Also, the density, the calorific value, and the volume flow of permanent gases are continuously analyzed and recorded. Gas samples are collected for the determination of the gas composition throughout the experiment. A gas chromatograph (GC) equipped with a thermal conductivity detector (TCD) and a flame ionization detector (FID) (Hewlett Packard, HP 5890A Series II) enables the quantitative measurement of the permanent gas composition (N₂, O₂, H₂, CO, CO₂, and the saturated and unsaturated hydrocarbons from C₁ to C₄). To validate the offline analysis online gas measurements are performed with a process GC (INFICON Micro GC Fusion) by quantification of the same gas species. To calculate the mass fraction of a gas species x_i , Eq. (1) is applied considering the gas density ρ_i while neglecting the purge gas. Non-quantifiable gases like remaining moisture or heteroatom-containing hydrocarbons are accounted for as 'others' on balance loss.

$$x_i = \frac{v_i \rho_i}{\sum v_z \rho_z} \quad (1)$$

$z = \text{H}_2, \text{CO}, \text{CO}_2, \text{CH}_4, \text{C}_2\text{H}_6, \text{C}_2\text{H}_4\text{C}_3\text{H}_8, \text{C}_3\text{H}_6, \text{C}_4\text{H}_{10}, \text{C}_4\text{H}_8, \text{others}$

The organic condensates are analyzed by GC combined with a FID (Agilent 7890B), which enables the quantification of the content of benzene, toluene, ethylbenzene, xylenes, styrene, phenol, ϵ -caprolactam, as well as 1-olefins and n -alkanes in the chain length ranging from C₅–C₂₁. The accumulated proportion of n -alkanes and 1-olefins in the range of C₅ to C₂₁ (PAO), like the accumulated share of benzene, toluene, ethylbenzene, xylenes, and styrene (BTEXS) is used as indicator for changes in the organic condensates. The water content is determined by Karl Fischer titration (Metrohm 870 KF Titrino Plus).

3 Results

3.1 Thermal vs. Catalytic Pyrolysis

Comparing thermal and catalytic experiments reveals the efficiency of the catalysts. Fig. 1 shows the product mass fractions generated in the experiments with different catalysts and W1 at 450 °C. The mass balance for the thermal pyrolysis of LDPE, PP, and W1 is also depicted. W1 is tested as a reference material because of its low content of impurities. In the thermal pyrolysis of both virgin polyolefins (LDPE and PP) mainly organic condensate is formed. In addition, a hydrocarbon-rich permanent gas is formed. Similar tendencies with a comparable amount of organic condensate and permanent gas can be obtained for the thermal pyrolysis of W1 despite higher balance losses. The condensates of LDPE and W1 are solid at room temperature, which indicates a large proportion of long-chain hydrocarbons similar to paraffin wax. In case of PP, a liquid organic condensate is formed. However, only a small amount of solid residue can be identified pyrolyzing LDPE and W1. The investigation of the solid residue reveals that it consists of polymeric residues and not of coke or other inorganic components, which indicates that at 450 °C and a solids residence time of 30 min, W1 and LDPE did not degrade completely in this reactor. Because of the expected high PE content in the agricultural films, an incomplete conversion (96 wt %) can be determined with both feedstocks. The condensates of LDPE and W1 are solid at room temperature, which indicates a large proportion of long-chain hydrocarbons similar to paraffin wax. In case of PP, a liquid organic condensate is formed.

A significant influence on product distribution occurs upon the addition of the catalyst. The zeolitic catalysts A and B lead to a significant reduction of the organic condensate yield in favour of the permanent gas. The organic

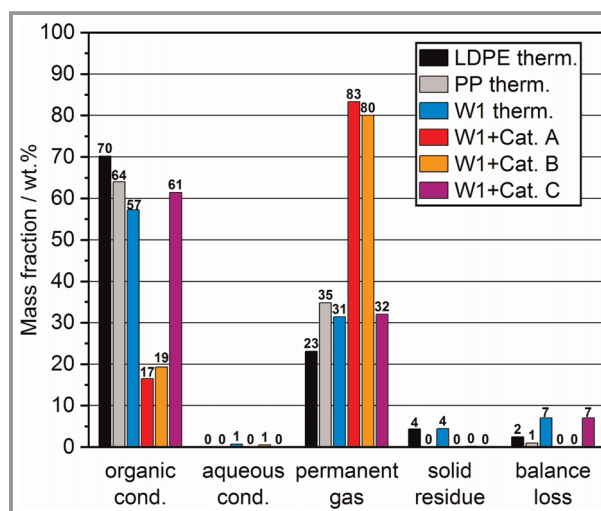


Figure 1. Mass balance of the thermal and in-situ catalytic pyrolysis of LDPE, PP, and W1 at 450 °C and a solid residence time of 30 min.

condensate obtained is liquid at room temperature. The addition of catalyst A increases the BTEXS content in the organic condensate from 0.3 wt% in the thermal test to 2.8 wt%. This effect is even more prominent with catalyst B (thermal 0.3 wt%, catalytic 7.9 wt%). The PAO decreases from the thermal test (25.2 wt%) to the experiments with catalyst A (6.6 wt%) and B (3.7 wt%). When catalyst C is involved in the reaction, the reduction of PAO is comparatively lower. No significant shift concerning the aromatic components occurs. Nevertheless, a minor influence can be identified regarding the organic condensate. The condensate, which is highly viscous at room temperature, has an aromatics content of 0.5 wt% and a PAO content of 8.2 wt% when catalyst C is used. Due to the enhanced cracking of long-chain paraffins a higher PAO is expected. However, a decline of the PAO is observed due to catalyst addition, which might be attributed to secondary reactions in the vapour phase ahead of the condensation. Isomerization reactions and aromatics formation are also promoted by the catalysts.

The changes in the gas composition for the thermal and catalytic pyrolysis of W1 are displayed in Fig. 2. While the thermal experiment yields a broad distribution of saturated to unsaturated gases, there is a clear shift towards olefins when the zeolitic catalysts are applied. More specifically, the zeolites lead to an increased formation of propene and butene. As expected, a relevant content of CO or CO₂ is not detectable in the not further specified remainder (“others”).

3.2 Feedstock Influence on Catalytic Pyrolysis

In catalytic pyrolysis, the impurities contained in the feedstock can deactivate the catalyst and thus reduce or even eliminate its cracking function [34]. Fig. 3 compares different feedstocks pyrolyzed with catalysts A and B at 450 °C and a solid residence time of 30 min. The low-contaminant

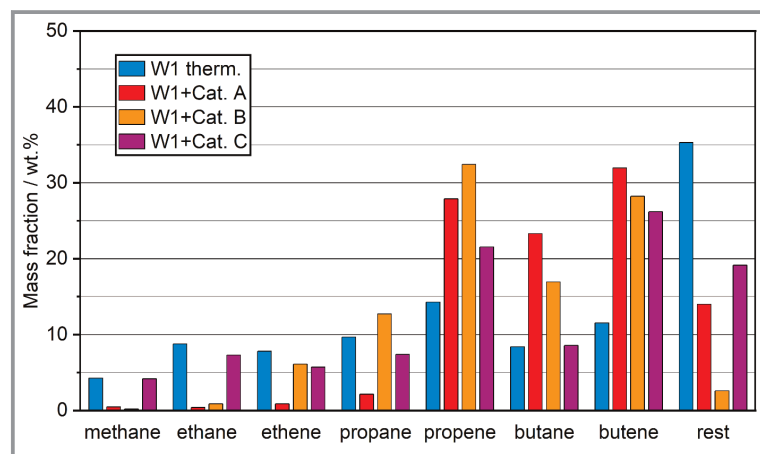


Figure 2. Hydrocarbon distribution in the permanent gas generated via thermal and catalytic pyrolysis W1 at 450 °C and a solid residence time of 30 min.

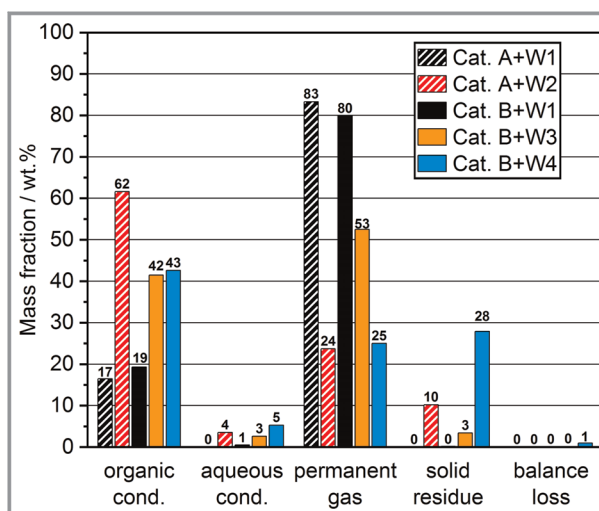


Figure 3. Mass balance of the in-situ catalytic pyrolysis of different feedstocks with catalysts A and B at 450 °C and a solid residence time of 30 min.

PIW W1 is employed as a reference. The study of W2, investigated with catalyst A, which contains oxygen and nitrogen, waxy organic condensate (60 wt%) similar to the results obtained in thermal LDPE-rich plastic pyrolysis is generated. In addition, significant solid residue formation is apparent. This residue consists of the sand particles and a black fine fraction, which, due to the low ash content in the feedstock, consists of coke. Furthermore, aqueous condensate is generated. CO₂ (27 wt%) and CO (7 wt%) can be detected in the product gas. The significant selectivity to propene and butene disappears. In the condensate, ϵ -caprolactam, the main product of polyamide 6 pyrolysis [46], is obtained with 6.5 wt%. The catalyst's characteristic formation of BTEXS is not observable. Thus, the heteroatom-containing polymers and the increased coke formation cause a significant deactivation of the catalyst. In particular, nitrogen can cause this deactivation [47], while oxygen in the feedstock promotes the formation of undesirable byproducts such as CO₂ or H₂O.

The two PCWs, W3 and W4, investigated with catalyst B, differ in composition from W2. The higher quality of W3, which contains fewer heteroatoms such as N and Cl, or non-organic compounds, results in less residual solids and a higher gas content. Both PCWs produce comparably low volumes of the aqueous condensate phase and yield 42–43 % of organic condensate. Particularly for W4, a complete deactivation of the catalyst is observed as can be seen by the low gas yield in combination with high solid residue production of 28 wt%. Again, the ash content of approx. 10 wt% in the feedstock indicates the significant formation of coke. Not shown here, the CO and CO₂ fractions account for 6 wt% and 49 wt% of the gaseous product from

W4, whereas the valuable olefinic gases reach 27 wt % due to the loss of catalytic selectivity. With 8.4 wt % of BETXS in the liquid product from W4, a comparable content to the experiment with W1 and catalyst B is detectable, which, however, may be attributed to the presence of polystyrene or similar structures rather than to a catalytic effect. A styrene content of 6.2 wt % supports this assumption since toluene and xylenes are preferentially formed during the catalytic formation of aromatics.

Comparing the results of W1 to W4, significantly less permanent gas and more solid residue can be detected the higher the nitrogen, oxygen, and chlorine content of the feedstocks are. In thermal pyrolysis, polyolefins and also polystyrene degrade almost without coke formation, in contrast to heteroatom-containing polymers or biomass. Nevertheless, the gas generated from W4 contains 9 wt % CO and 44 wt % CO₂. The condensate exists in form of wax at room temperature, which further indicates the deactivation of the catalyst during the pyrolysis process despite the higher quality of the feedstock.

3.3 Influence of Process Temperature and Solids Residence Time

A higher reactor temperature increases the chemical reaction rate. Neglecting heat and mass transfer limitations of the reactor, the application of a suitable catalyst can accelerate the reaction and thus reduce the reactor temperature needed for full feedstock conversion.

The mass balance of the pyrolysis of W1 and catalyst A at different pyrolysis temperatures and solids residence times is shown in Fig. 4. With a reduction from 550 °C to 450 °C, only a slight shift from permanent gases to organic condensate is detectable in the product distribution. At the same time, a small amount of solid residue can be detected at 550 °C, which may be caused by an increased tendency to coke formation. The effect of an enhanced cracking reaction and coke formation due to higher temperature has already been reported consistent in the literature [48]. If the reaction temperature is further reduced to 400 °C, 19 wt % of solid residue is observed. In this case, the temperature is insufficient for complete conversion of the feedstock although the catalyst is added at a residence time in the reactor chamber is 30 min. By increasing the solids residence time to 60 min, the conversion can be enhanced to 95 wt %. At 400 °C and 60 min significantly fewer gaseous hydrocarbons are formed and more organic condensate is generated. If the reaction temperature is reduced to 380 °C, the degree of conversion continues to decline, as expected.

The gas composition of the experiments with almost complete conversion (550 °C and 30 min, 450 °C and 30 min, 400 °C and 60 min) reveals

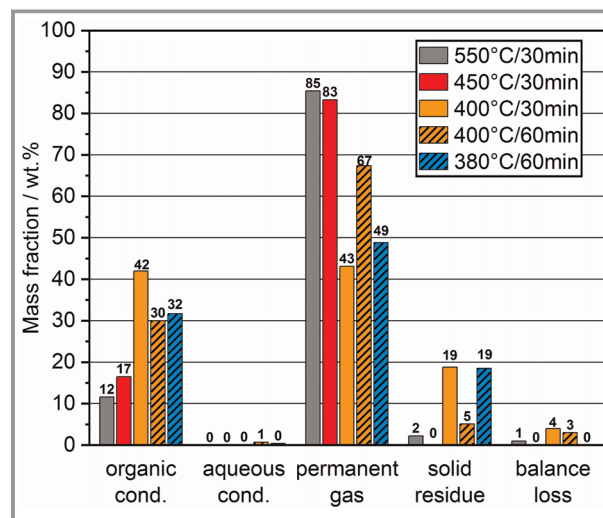


Figure 4. Mass balance of the in-situ catalytic pyrolysis of W1 with catalyst A at varying temperatures and solid residence times.

an effect on product distribution, as can be seen in Fig. 5. While relevant amounts of methane (10.3 wt %) and ethane (5.1 wt %) are produced at 550 °C, these hydrocarbons accumulate to only 0.9 wt % and 1.9 wt % at 450 °C and 400 °C, respectively. At a low reactor temperature of 400 °C, ethene, propene, and butene sum up to 84 wt % of total permanent gas, while at 450 °C approx. 61 wt % and at 550 °C 59 wt % are generated. This effect may be attributed to the superposition of thermal and catalytic cracking within the reaction system.

A significant shift of the compositions also occurs in the condensate. From 4.9 wt % of the condensate for the experiments at 400 °C, the PAO increases to 7.4 wt % at 550 °C, while the distribution within the chain length C₅ to C₂₁ remains consistent. However, in the 550 °C experiment with catalyst A, significantly higher BTEXS are measured with

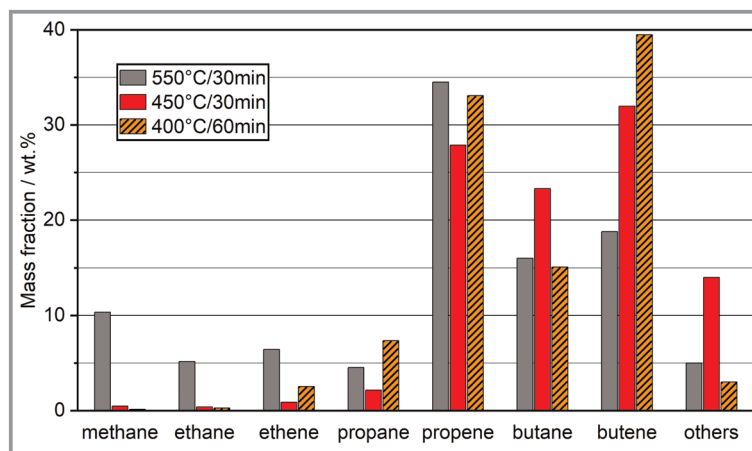


Figure 5. Hydrocarbon distribution in the permanent gas generated via catalytic pyrolysis of W1 with catalyst A at varying temperatures and solid residence times.

11.5 wt % compared to the 400 °C experiment (2.0 wt %). Supposedly, a higher reactor temperature results in a stronger tendency to secondary reactions of primary products in the reaction chamber [49].

3.4 Catalyst Fixation, Deactivation and Regeneration

Catalyst deactivation resulting from occupied active acidic sites due to coke deposition or catalyst poisoning is an important effect related to catalyst consumption [34]. Coke deposition can be removed by suitable catalyst regeneration, thus preparing the catalyst for repetitive operation [35]. However, this requires a permanent fixation of the catalyst on the sand surface which is achieved by the preparation method with silica binder. In Fig. 6, the results of the catalyst-sand mixture prepared with paraffin binder and silica-based binder are compared for both zeolitic catalysts. For both preparation methods, similar experimental results are obtained indicating that catalyst fixation has no impact on its activity.

Applying catalyst B', regeneration by coke combustion was investigated based on W1. Because of the W1 composition, poisoning as a result of heteroatom-containing hydrocarbons should be negligible. The catalyst-sand mixture is used twice after the first and again after the second pyrolysis test run for catalytic pyrolysis without further treatment. Regeneration follows the three test runs. For this purpose, the catalyst-sand mixture was placed in an oven at 600 °C in an oxygen-rich atmosphere for 6 h. Before the material is reused in regenerated form, ash particles down to 500 µm were removed by sieving. During the process, relevant changes in the sand-catalyst ratio can be neglected due to the low relative velocities of the particles in the reactor. As a consequence of catalyst reuse the gas formation decreases in

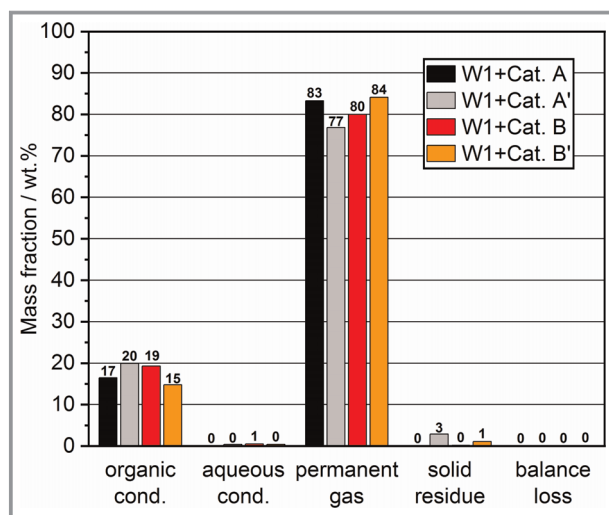


Figure 6. Mass balance of the in-situ catalytic pyrolysis of W1 with catalysts A, A', B, and B' at 450 °C and a solid residence time of 30 min.

favour of the organic condensate fraction, like shown in Fig. 7. In addition, coke formation is enhanced. After regeneration, a gas yield similar to the experiment with unused catalyst B' is obtained, while changes in the composition of the condensates are detectable. The multiple uses of catalyst B' without regeneration diminish the characteristic formation of BTEXS captured as organic condensate significantly whereas the amount of PAO increases slightly. Thus, in the test with unused catalyst B', the BTEXS accounts for 10.9 wt %, but after three repeated runs for only 0.7 wt %. The PAO content increases by approx. 60 % from the first run (3.5 wt %). After regeneration, the PAO is decreasing and more BTEXS can be obtained. However, the composition is more comparable to the organic condensate after single reuse than to that of new catalyst B'. The results indicate the feasibility of catalyst regeneration if prepared with silica binder in case of deactivation by coking.

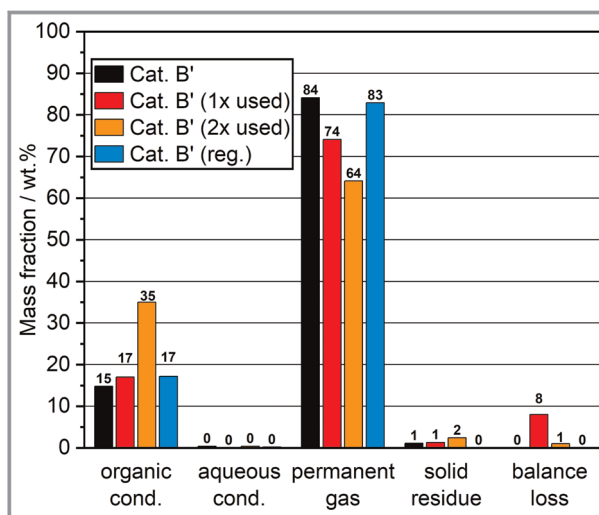


Figure 7. Mass balance of the in-situ catalytic pyrolysis of W1 with new, used, and regenerated catalysts B' at 450 °C and a solid residence time of 30 min.

4 Conclusions and Outlook

The results in this work demonstrate the potential of in-situ catalytic pyrolysis for recycling polyolefin-rich plastic waste with a focus on producing light olefins. In accordance to other studies [16, 27, 28], the results indicate a significant promotion of the cracking and secondary reactions by zeolitic catalysts. A distinctive characteristic demonstrated by the process is reduced coke formation of less than 3 wt % in the catalytic slow pyrolysis of polyolefinic waste with small contamination content. Thus, the successful development of the catalyst preparation and its use for catalytic pyrolysis at a technical scale is demonstrated in an auger-type reactor. Permanent silica fixation of the catalyst allows multiple utilization and enables regeneration upon deactivation by coke deposition. Catalyst deactivation caused by feedstocks, especially by nitrogen-containing components, significantly

reduces the process efficiency. However, complete pyrolytic conversion can be achieved with zeolites even under mild conditions of 450 °C and with a solids residence time of 30 min for PIW which feature low heteroatom content in contrast to thermal pyrolysis. In this case, high product recycling rates in form of light olefins up to 56 wt.% are estimated.

Catalytic pyrolysis of polyolefin-rich PIW generates a significant amount of ethene, propene, and butenes, which, if adequately purified, can be recycled to produce new virgin-quality plastics [50, 51]. The reduced tendency towards the formation of coke as unwanted by-product also increases the process efficiency. By incorporating a pyrolysis plant into a petrochemical production site, both, the hydrocarbon-rich gases and the organic condensates can be used after suitable upgrading [52]. Pyrolysis oil upgrading through hydrotreatment can include removal of chemically bound heteroatoms, adaption of the boiling curve, and reduction of the olefin content. Naphtha and middle distillate produced in the oil refinement are potential feedstocks for steam cracking (SC) assuming heteroatoms and inorganic impurities can be detached to fulfill the SC process feedstock specification [53]. Ethene, propene, butenes, and butadienes, are produced via the SC route [54, 55]. The main catalytic pyrolysis product, pyrolysis gas rich in C₂–C₄ olefins, can directly undergo thermal separation to gain the desired SC products, e.g., through introduction into the cold section of the SC process. Therefore, further investigations on catalytic pyrolysis of polyolefin-rich plastic waste must include characterization of gaseous and liquid products in terms of heteroatoms. In addition, long term stability investigation on catalyst use and regeneration as a function of waste heteroatom content would be necessary to determine a catalyst substitution rate.

Author contribution

N. Netsch: Conceptualization, literature study, experimental investigation, analytics, data analysis, manuscript writing. J. Vogt: Literature study, data analysis, manuscript writing. F. Richter: Conceptualization, experimental investigation. G. Straczewski: Analytics, review & editing. G. Mannebach: Feedstock preparation. V. Fraaije: Catalyst preparation, review & editing. S. Tavakkol: Conceptualization. S. Mihan: Conceptualization, review & editing. D. Stapf: Conceptualization, review & editing.

Acknowledgment

The authors thank Basell Polyolefine GmbH for providing the feedstock material and the catalysts for this study, as well as for its financial and organizational support of this work. In addition, the authors acknowledge Hans Leibold and Marco Tomasi-Morgano for their contribution to previous studies. Open access funding enabled and organized by Projekt DEAL.

Symbols used

x	[-]	mass fraction
v	[-]	volume fraction
ρ	[kg m ⁻³]	density

Abbreviations

BTEXS	benzene, toluene, ethylbenzene, xylenes, and styrene
EVOH	ethylene vinyl alcohol
FCC	fluid catalytic cracking
FID	flame ionization detector
GC	gas chromatograph / gas chromatography
HDPE	high-density polyethylene
LPG	liquefied petroleum gas (propane-butane mixture)
LDPE	low-density polyethylene
PAO	proportion of <i>n</i> -alkanes and 1-olefins in the permanent gas
PCW	post-consumer waste
PET	polyethylene terephthalate
PIW	post-industrial waste
PP	polypropylene
SC	steam cracker / steam cracking
TCD	thermal conductivity detector
W1	post-industrial waste of agricultural films
W2	post-industrial waste of multilayer packaging films
W3	polyolefin-rich fraction of mixed plastic waste from mechanical recycling
W4	light fraction of mixed plastic waste generated by mechanical sorting

References

- [1] M. Humphreys, *J. Conflict Resolut.* **2005**, *49* (4), 508–537. DOI: <https://doi.org/10.1177/0022002705277545>
- [2] *Global Warming of 1.5°C* (Eds: Valérie Masson-Delmotte et al.) IPCC, Cambridge University Press, Cambridge **2022**. <https://www.cambridge.org/core/books/global-warming-of-15c/D7455D42B4C820E706A03A169B1893FA>
- [3] M. A. Camilleri, *Sustainable Dev.* **2020**, *28* (6), 1804–1812. DOI: <https://doi.org/10.1002/sd.2113>
- [4] T. Domenech, B. Bahn-Walkowiak, *Ecol. Econ.* **2019**, *155*, 7–19. DOI: <https://doi.org/10.1016/j.ecolecon.2017.11.001>
- [5] P. Wang, S. Kara, *Procedia CIRP* **2019**, *80*, 667–672. DOI: <https://doi.org/10.1016/j.procir.2019.01.056>
- [6] C. H. Christensen, J. Rass-Hansen, C. C. Marsden, E. Taarning, K. Egeblad, *ChemSusChem* **2008**, *1* (4), 283–289. DOI: <https://doi.org/10.1002/cssc.200700168>
- [7] M. Aresta, A. Dibenedetto, *Dalton Trans.* **2007**, *28*, 2975–2992. DOI: <https://doi.org/10.1039/b700658f>
- [8] T. Keijer, V. Bakker, J. C. Sloopweg, *Nat. Chem.* **2019**, *11* (3), 190–195. DOI: <https://doi.org/10.1038/s41557-019-0226-9>
- [9] *Global Plastics Outlook*, OECD Publishing, Paris **2022**.
- [10] *Plastics – The Facts 2020. An analysis of European plastics production, demand and waste data*, PlasticsEurope, Brussels **2020**.
- [11] K. Ragaert, L. Delva, K. van Geem, *Waste Manage.* **2017**, *69*, 24–58. DOI: <https://doi.org/10.1016/j.wasman.2017.07.044>
- [12] O. Dogu, M. Pelucchi, R. van de Vijver, P. H. van Steenberge, D. R. D'hooge, A. Cuoci, M. Mehl, A. Frassoldati, T. Faravelli,

- K. M. van Geem, *Prog. Energy Combust. Sci.* **2021**, *84*, 100901. DOI: <https://doi.org/10.1016/j.pecs.2020.100901>
- [13] A. Rahimi, J. M. Garcia, *Nat. Rev. Chem.* **2017**, *1*, 0046. DOI: <https://doi.org/10.1038/s41570-017-0046>
- [14] I. Vollmer, M. J. F. Jenks, M. C. P. Roelands, R. J. White, T. van Harmelen, P. de Wild, G. P. van der Laan, F. Meirer, J. T. F. Keurentjes, B. M. Weckhuysen, *Angew. Chem., Int. Ed.* **2020**, *59* (36), 15402–15423. DOI: <https://doi.org/10.1002/anie.201915651>
- [15] P. Quicker, M. Seitz, J. Vogel, *Waste Manage. Res.* **2022**, *40* (10), 1494–1504. DOI: <https://doi.org/10.1177/0734242X221084044>
- [16] D. P. Serrano, J. Aguado, J. M. Escola, *ACS Catal.* **2012**, *2* (9), 1924–1941. DOI: <https://doi.org/10.1021/cs3003403>
- [17] P. J. Donaj, W. Kaminsky, F. Buzeto, W. Yang, *Waste Manage.* **2012**, *32* (5), 840–846. DOI: <https://doi.org/10.1016/j.wasman.2011.10.009>
- [18] W. Kaminsky, I.-J. N. Zorriquetta, *J. Anal. Appl. Pyrolysis* **2007**, *79* (1–2), 368–374. DOI: <https://doi.org/10.1016/j.jaap.2006.11.005>
- [19] Y. Zhang, Z. Fu, W. Wang, G. Ji, M. Zhao, A. Li, *ACS Sustainable Chem. Eng.* **2022**, *10* (1), 91–103. DOI: <https://doi.org/10.1021/acsschemeng.1c04915>
- [20] M. S. Abbas-Abadi, Y. Ureel, A. Eschenbacher, F. H. Vermeire, R. J. Varghese, J. Oenema, G. D. Stefanidis, K. M. van Geem, *Prog. Energy Combust. Sci.* **2023**, *96*, 101046. DOI: <https://doi.org/10.1016/j.pecs.2022.101046>
- [21] T. Maqsood, J. Dai, Y. Zhang, M. Guang, B. Li, *J. Anal. Appl. Pyrolysis* **2021**, *159*, 105295. DOI: <https://doi.org/10.1016/j.jaap.2021.105295>
- [22] S. M. Al-Salem, A. Antelava, A. Constantinou, G. Manos, A. Dutta, *J. Environ. Manage.* **2017**, *197*, 177–198. DOI: <https://doi.org/10.1016/j.jenvman.2017.03.084>
- [23] D. K. Ratnasari, M. A. Nahil, P. T. Williams, *J. Anal. Appl. Pyrolysis* **2017**, *124*, 631–637. DOI: <https://doi.org/10.1016/j.jaap.2016.12.027>
- [24] V. Daligaux, R. Richard, M.-H. Manero, *Catalysts* **2021**, *11* (7), 770. DOI: <https://doi.org/10.3390/catal11070770>
- [25] C. R. Marcilly, *Top. Catal.* **2000**, *13* (4), 357–366. DOI: <https://doi.org/10.1023/A:1009007021975>
- [26] K.-H. Lee, S.-G. Jeon, K.-H. Kim, N.-S. Noh, D.-H. Shin, J. Park, Y. Seo, J.-J. Yee, G.-T. Kim, *Korean J. Chem. Eng.* **2003**, *20* (4), 693–697. DOI: <https://doi.org/10.1007/BF02706909>
- [27] Y.-H. Lin, M.-H. Yang, T.-F. Yeh, M.-D. Ger, *Polym. Degrad. Stab.* **2004**, *86* (1), 121–128. DOI: <https://doi.org/10.1016/j.polydegradstab.2004.02.015>
- [28] F. Pinto, P. Costa, I. Gulyurtlu, I. Cabrita, *J. Anal. Appl. Pyrolysis* **1999**, *51* (1–2), 57–71. DOI: [https://doi.org/10.1016/S0165-2370\(99\)00008-X](https://doi.org/10.1016/S0165-2370(99)00008-X)
- [29] G. Manos, A. Garforth, J. Dwyer, *Ind. Eng. Chem. Res.* **2000**, *39* (5), 1198–1202. DOI: <https://doi.org/10.1021/ie990512q>
- [30] E. Butler, G. Devlin, K. McDonnell, *Waste Biomass Valorization* **2011**, *2* (3), 227–255. DOI: <https://doi.org/10.1007/s12649-011-9067-5>
- [31] S. D. Anuar Sharuddin, F. Abnisa, W. M. A. Wan Daud, M. K. Aroua, *Energy Convers. Manage.* **2016**, *115*, 308–326. DOI: <https://doi.org/10.1016/j.enconman.2016.02.037>
- [32] N. Chaouati, A. Soualah, I. Hussein, J.-D. Comparot, L. Pinard, *Appl. Catal., A* **2016**, *526*, 95–104. DOI: <https://doi.org/10.1016/j.apcata.2016.08.004>
- [33] Y. Sakata, M. Azhar Uddin, A. Muto, Y. Kanada, K. Koizumi, K. Murata, *J. Anal. Appl. Pyrolysis* **1997**, *43* (1), 15–25. DOI: [https://doi.org/10.1016/S0165-2370\(97\)00052-1](https://doi.org/10.1016/S0165-2370(97)00052-1)
- [34] H. S. Cerqueira, G. Caeiro, L. Costa, F. Ramôa Ribeiro, *J. Mol. Catal. A: Chem.* **2008**, *292* (1–2), 1–13. DOI: <https://doi.org/10.1016/j.molcata.2008.06.014>
- [35] A. López, I. de Marco, B. M. Caballero, A. Adrados, M. F. Laresgoiti, *Waste Manage.* **2011**, *31* (8), 1852–1858. DOI: <https://doi.org/10.1016/j.wasman.2011.04.004>
- [36] S. Ali, A. Garforth, D. Harris, D. Rawlence, Y. Uemichi, *Catal. Today* **2002**, *75* (1–4), 247–255. DOI: [https://doi.org/10.1016/S0920-5861\(02\)00076-7](https://doi.org/10.1016/S0920-5861(02)00076-7)
- [37] A. Garforth, Y.-H. Lin, P. Sharratt, J. Dwyer, *Appl. Catal., A* **1998**, *169* (2), 331–342. DOI: [https://doi.org/10.1016/S0926-860X\(98\)00022-2](https://doi.org/10.1016/S0926-860X(98)00022-2)
- [38] D. Serrano, *Appl. Catal., B* **2004**, *49* (4), 257–265. DOI: <https://doi.org/10.1016/j.apcatb.2003.12.014>
- [39] A. Marcilla, A. Gómez-Siurana, D. Berenguer, *Appl. Catal., A* **2006**, *301* (2), 222–231. DOI: <https://doi.org/10.1016/j.apcata.2005.12.018>
- [40] R. Miandad, M. Rehan, M. A. Barakat, A. S. Aburiazaiza, H. Khan, I. M. I. Ismail, J. Dhavamani, J. Gardy, A. Hassanpour, A.-S. Nizami, *Front. Energy Res.* **2019**, *7*. DOI: <https://doi.org/10.3389/fenrg.2019.00027>
- [41] N. Miskolczi, F. Ateş, N. Borsodi, *Bioresour. Technol.* **2013**, *144*, 370–379. DOI: <https://doi.org/10.1016/j.biortech.2013.06.109>
- [42] C. Muhammad, J. A. Onwudili, P. T. Williams, *J. Anal. Appl. Pyrolysis* **2015**, *113*, 332–339. DOI: <https://doi.org/10.1016/j.jaap.2015.02.016>
- [43] N. Netsch, M. Simons, A. Feil, H. Leibold, F. Richter, J. Slama, S. P. Yogish, K. Greiff, D. Stapf, *Waste Manage.* **2022**, *150*, 141–150. DOI: <https://doi.org/10.1016/j.wasman.2022.07.001>
- [44] M. Tomasi Morgano, H. Leibold, F. Richter, H. Seifert, *J. Anal. Appl. Pyrolysis* **2015**, *113*, 216–224. DOI: <https://doi.org/10.1016/j.jaap.2014.12.019>
- [45] M. Zeller, N. Netsch, F. Richter, H. Leibold, D. Stapf, *Chem. Ing. Tech.* **2021**, *93* (11), 1763–1770. DOI: <https://doi.org/10.1002/cite.202100102>
- [46] H. Bockhorn, S. Donner, M. Gernsbeck, A. Hornung, U. Hornung, *J. Anal. Appl. Pyrolysis* **2001**, *58–59*, 79–94. DOI: [https://doi.org/10.1016/S0165-2370\(00\)00187-X](https://doi.org/10.1016/S0165-2370(00)00187-X)
- [47] X. Chen, Y. Liu, S. Li, X. Feng, H. Shan, C. Yang, *Energy Fuels* **2017**, *31* (4), 3659–3668. DOI: <https://doi.org/10.1021/acs.energyfuels.6b03230>
- [48] V. Cozzani, C. Nicoletta, M. Rovatti, L. Tognotti, *Ind. Eng. Chem. Res.* **1997**, *36* (2), 342–348. DOI: <https://doi.org/10.1021/ie950779z>
- [49] R. W. J. Westerhout, J. A. M. Kuipers, W. P. M. van Swaaij, *Ind. Eng. Chem. Res.* **1998**, *37* (3), 841–847. DOI: <https://doi.org/10.1021/ie970384a>
- [50] M. Seitz, S. Schröter, *Chem. Ing. Tech.* **2022**, *94* (5), 720–726. DOI: <https://doi.org/10.1002/cite.202100182>
- [51] A. Somoza-Tornos, A. Gonzalez-Garay, C. Pozo, M. Graells, A. Espuña, G. Guillén-Gosálbez, *ACS Sustain. Chem. Eng.* **2020**, *8* (9), 3561–3572. DOI: <https://doi.org/10.1021/acsschemeng.9b04835>
- [52] P. Neuner, D. Graf, N. Netsch, M. Zeller, T.-C. Herrmann, D. Stapf, R. Rauch, *Reactions* **2022**, *3* (3), 352–373. DOI: <https://doi.org/10.3390/reactions3030026>
- [53] M. Kusenberg, A. Eschenbacher, M. R. Djokic, A. Zayoud, K. Ragaert, S. de Meester, K. M. van Geem, *Waste Manage.* **2022**, *138*, 83–115. DOI: <https://doi.org/10.1016/j.wasman.2021.11.009>
- [54] M. Kusenberg, G. C. Fausson, H. D. Thi, M. Roosen, M. Grilc, A. Eschenbacher, S. de Meester, K. M. van Geem, *Sci. Total Environ.* **2022**, *838* (Pt 2), 156092. DOI: <https://doi.org/10.1016/j.scitotenv.2022.156092>
- [55] M. Kusenberg, M. Roosen, A. Zayoud, M. R. Djokic, H. Dao Thi, S. de Meester, K. Ragaert, U. Kresovic, K. M. van Geem, *Waste Manage.* **2022**, *141*, 104–114. DOI: <https://doi.org/10.1016/j.wasman.2022.01.033>

DOI: 10.1002/cite.202300078

Chemical Recycling of Polyolefinic Waste to Light Olefins by Catalytic Pyrolysis

Niklas Netsch, Jonas Vogt, Frank Richter, Grazyna Straczewski, Gerd Mannebach, Volker Fraaije, Salar Tavakkol*, Shahram Mihan, Dieter Stapf

Research Article: The conversion of polyolefin-rich plastic waste into unsaturated gaseous hydrocarbons enables polyolefin-to-olefin recycling. Experimental investigations of in-situ catalytic pyrolysis in a pilot-scale auger-type reactor reveal the significant potential to increase recycling rates but also show current processing and feedstock hurdles.

